Journal of Electromyography and Kinesiology 74 (2024) 102850

Contents lists available at ScienceDirect

Journal of Electromyography and Kinesiology

journal homepage: www.elsevier.com/locate/jelekin

Tutorial: Analysis of central and peripheral motor unit properties from decomposed High-Density surface EMG signals with *openhdemg*

Giacomo Valli [a,b,*], Paul Ritsche [c], Andrea Casolo [a], Francesco Negro [b], Giuseppe De Vito [a]

[a] Department of Biomedical Sciences, University of Padova, Padova, Italy
[b] Department of Clinical and Experimental Sciences, University of Brescia, Brescia, Italy
[c] Department of Sport, Exercise and Health, University of Basel, Basel, Switzerland

ARTICLE INFO

Keywords:
High-Density surface EMG
Motor units
Signal processing
Python
Open-source

ABSTRACT

High-Density surface Electromyography (HD-sEMG) is the most established technique for the non-invasive analysis of single motor unit (MU) activity in humans. It provides the possibility to study the central properties (e.g., discharge rate) of large populations of MUs by analysis of their firing pattern. Additionally, by spike-triggered averaging, peripheral properties such as MUs conduction velocity can be estimated over adjacent regions of the muscles and single MUs can be tracked across different recording sessions. In this tutorial, we guide the reader through the investigation of MUs properties from decomposed HD-sEMG recordings by providing both the theoretical knowledge and practical tools necessary to perform the analyses. The practical application of this tutorial is based on *openhdemg*, a free and open-source community-based framework for the automated analysis of MUs properties built on Python 3 and composed of different modules for HD-sEMG data handling, visualisation, editing, and analysis. *openhdemg* is interfaceable with most of the available recording software, equipment or decomposition techniques, and all the built-in functions are easily adaptable to different experimental needs. The framework also includes a graphical user interface which enables users with limited coding skills to perform a robust and reliable analysis of MUs properties without coding.

1. Introduction

The motor unit (MU) is the basic functional component of the neuromuscular system that consists of an alpha motoneuron, its axon, and the muscle fibres it innervates (Heckman and Enoka, 2012; Sherrington, 1925). The central nervous system (CNS) responds to the locomotor functional demands by sending trains of axonal discharges (i.e. neural information or activation signal), which in turn elicit action potentials in the innervated muscle fibres (i.e. MUs action potentials (MUAPs)) (Heckman and Enoka, 2012, 2004). In simple terms, MUs act as a transducer that converts the neural activation signal into muscular forces. Indeed, because of a large physiological safety factor in synaptic transmission at the neuromuscular junction (Sarto et al., 2022a; Wood and Slater, 2001), there is a one-to-one relation between the discharges of a motoneuron and the MUAPs evoked in the muscle (Duchateau and Enoka, 2011; Wood and Slater, 2001).

During voluntary muscle contractions, the MUAPs can be detected at the muscle level via electromyographic (EMG) recordings, therefore making the motoneurons the only cells of the CNS that can be recorded in humans with non-invasive or minimally-invasive techniques (Farina et al., 2004; Merletti and Farina, 2009). Recent advancements in EMG techniques have led to the development of High-Density surface EMG (HD-sEMG), where densely populated grids of closely spaced small-diameter recording electrodes are applied directly to the skin overlying the muscles (Gallina et al., 2022). The elevated spatial sampling of these grids allowed the researchers to record MUAPs from different

Abbreviations: CNS, Central Nervous System; COVisi, Coefficient of variation of Interspike interval; DR, Discharge Rate; EMG, Electromyography; HD-EMG, High-Density Electromyography; HD-sEMG, High-Density surface Electromyography; iEMG, Intramuscular Electromyography; ISI, Interspike interval; MUAP, Motor Units Action Potential; MU, Motor Unit; MUCV, Motor Unit Conduction Velocity; MVC, Maximum Voluntary Contraction; PNR, Pulse to Noise Ratio; PPS, Pulse Per Second; RMS, Root Mean Square; SIL, Silhouette Score; XCC, Cross-Correlation Coefficient.

* Corresponding author at: Neuromuscular Physiology Laboratory, Department of Biomedical Sciences, University of Padova, via F. Marzolo 3, 35131, Padova, Italy.

E-mail addresses: giacomo.valli@phd.unipd.it (G. Valli), paul.ritsche@unibas.ch (P. Ritsche), andrea.casolo@unipd.it (A. Casolo), francesco.negro@unibs.it (F. Negro), giuseppe.devito@unipd.it (G. De Vito).

https://doi.org/10.1016/j.jelekin.2023.102850
Received 20 July 2023; Received in revised form 5 October 2023; Accepted 28 November 2023
Available online 30 November 2023

regions of the muscle, thus increasing the possibility to discriminate spatially non-overlapping MUAPs and the number of single MUs that could be accurately decomposed (Farina et al., 2016). These advancements allowed for the simultaneous discrimination of large and representative populations of concurrently active MUs without invasive procedures (Farina et al., 2016).

These peculiar features established HD-sEMG as the preferred tool for researchers in physiology, sports science and medicine to investigate how the CNS controls voluntary movements in physiological conditions, and opened a new era in the study of MUs physiology and activity in response to different stimuli (Casolo et al., 2021; Martinez-Valdes et al., 2018; Škarabot et al., 2023; Valli et al., 2023), in health and pathology (Drost et al., 2001; Gallego et al., 2015), to injury (Nuccio et al., 2021) and for man–machine interface applications (Farina et al., 2017).

In this tutorial, we provide the reader with the theoretical knowledge necessary to perform a complete investigation of central and peripheral MUs properties such as MUs recruitment/derecruitment thresholds, discharge rate, and conduction velocity from decomposed HD-sEMG recordings. Additionally, in this context we introduce *openhdemg*, an innovative, freely available, and open-source framework specifically designed for the automated analysis of MU properties in decomposed HD-EMG recordings (Fig. 1).

2. Lowering the barriers to the use of HD-sEMG with *openhdemg*

Although some general consensus and standardisation on HD-sEMG data acquisition and analysis has been recently proposed (Gallina et al., 2022; Martinez-Valdes et al., 2023), the implementation of this technique still faces notable challenges. One such challenge is the limited availability of practical guidelines, instructions and user-friendly open-source software for the analysis of MUs activity (Felici and Del Vecchio, 2020). Indeed, proper analysis of HD-sEMG recordings requires specialized knowledge and expertise in signal processing and computational methods, alongside advanced coding skills, which may preclude some laboratories from such type of research.

The aim of this tutorial article is to lower some of the barriers to the implementation of the HD-sEMG technique by providing the reader with the theoretical knowledge and practical tools necessary to investigate MUs properties from decomposed HD-sEMG recordings.

Specifically, this tutorial has been structured as a step-by-step guide to the analysis of central and peripheral MUs properties once the discharge times are known, and combines simple and clear guidelines with an easy-to-read code implementation of all the showed concepts.

The tutorial will briefly cover basic concepts of signal acquisition and decomposition (as these phases generate the information to be analysed) and will then cover, in detail, the following steps:

- Load the decomposed HD-sEMG file in a working environment;
- Visualise, inspect and process the decomposition outcome;
- Discard unwanted MUs based on objective criteria;
- Track MUs within and between recording sessions;
- Analyse central and peripheral MUs properties;

For organisational purposes, the main text of the manuscript will focus on the theoretical aspects necessary to correctly investigate MUs activity. Alongside the text, figures and figures' captions will illustrate the application of all the discussed notions. Furthermore, a clear and in-depth documentation of the code implementation will allow the users to interactively follow all the steps of this tutorial and to implement their own analyses.

The practical application of the tutorial can be easily followed by readers with any scientific background and no advanced or strong knowledge of signal processing and coding will be required.

In order to achieve or purpose, we will use *openhdemg*, a free and open-source framework specifically designed for the analysis of MUs properties from HD-EMG recordings. *openhdemg* is written in Python 3

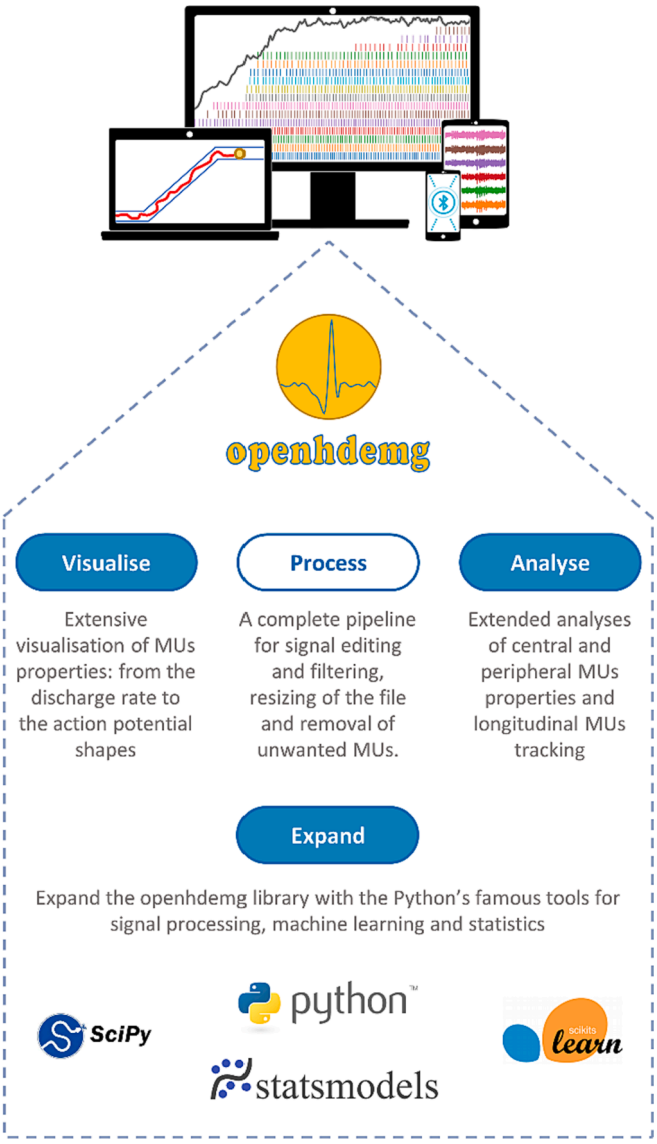

Fig. 1. The *openhdemg* framework. *openhdemg* is a free, versatile and open-source framework for the analysis of single motor unit (MU) properties from High-Density Electromyography (HD-EMG) recordings. It can be virtually interfaced with any custom or commercial system for HD-EMG data acquisition and decomposition. Starting from the discharge pattern of the identified MUs, *openhdemg* automates the steps of visualisation, processing and analysis of the decomposed HD-EMG file. Developed using Python 3, a widely recognized programming language for data analysis, *openhdemg* provides a rich set of built-in functions that can be further expanded using popular tools for signal processing, machine learning, and statistics available in the Python ecosystem.

(Python Software Foundation, USA) and, at the time of writing, it is composed of 9 modules and 75 functions for HD-EMG data handling, visualisation, editing and analysis easily adaptable to different experimental needs (Fig. 1). All the functions are designed for the maximum simplicity and convenience of the user and are extensively documented at https://www.giacomovalli.com/openhdemg/.

Noticeably, *openhdemg* is designed to be interfaced with any available system for data acquisition and decomposition, starting from the commercially available software up to any personal implementation of these phases, with little or no customisation required by the user.

For didactic purpose, the user is encouraged to follow the tutorial article with the provided code implementation of all the showed concepts. This approach enables users to directly utilise the individual functions within the *openhdemg* framework. These functions are

designed to offer maximum customization and flexibility, allowing for further extension with well-known Python libraries dedicated to signal processing and data analysis (as depicted in Fig. 1). By doing so, users can leverage their ability to perform advanced investigations.

However, the reader can also decide to use the built-in graphical user interface (presented in Fig. 2), which enables users to perform analysis tasks with ease and efficiency without writing a single line of code. The graphical interface contains all the tools needed to follow this tutorial article and to analyse MUs properties in real-life scenarios. For the interested readers, the use of the graphical interface is well documented at (https://www.giacomovalli.com/openhdemg/gui_intro/).

3. Fundamentals of HD-sEMG signal acquisition and decomposition

Although the explanation of procedures for HD-sEMG signal acquisition and decomposition into MUs discharge patterns goes beyond the scope of this article, these are the prerequisites for generating the output that is subsequently analysed, and are determinant for the quality of the analysis. Therefore, the following two sections are intended to provide a brief overview of the fundamental concepts for HD-sEMG data acquisition and decomposition in light of the subsequent analyses. For the readers that need further explanations, we redirect to more specialised articles covering these topics (Besomi et al., 2019; Del Vecchio et al., 2020; McManus et al., 2020; Merletti and Cerone, 2020; Merletti and Muceli, 2019). Additionally, Fig. 3 provides a visual representation of the key steps in HD-sEMG signal acquisition and decomposition in light of the subsequent analyses.

3.1. Signal acquisition

Being the primary step of all the studies involving HD-sEMG recordings, the signal acquisition phase will determine the type of analysis that can be performed, the number of accurately identified MUs and the reliability of the obtained results.

According to recent consensus (Gallina et al., 2022), if the scope is to investigate both central and peripheral properties of single MUs, the HD-sEMG signal should be recorded during isometric contractions (Fig. 3A–C) with densely populated grids of closely spaced (2.5 – 10 mm) electrodes of small diameter (0.5 – 3 mm). Additionally, the number and distribution of the recording electrodes should be adequate to accurately represent the propagation of MUAPs through the muscle fibres. Nowadays, it is common practice to use 32 or more recording electrodes, especially on large muscles (Cohen et al., 2023; Del Vecchio et al., 2017; Okudaira et al., 2023).

Given that HD-sEMG signals have a bandwidth of approximately 10–500 Hz, the signal should be preferentially recorded with a sampling rate of at least 2000 Hz (McManus et al., 2020). Additionally, the signal should be recorded in monopolar configuration (montage), in order to maximise the information that can be collected and to allow for different off-line spatial filtering (e.g., single or double differential) (Fig. 3G) (Gallina et al., 2022).

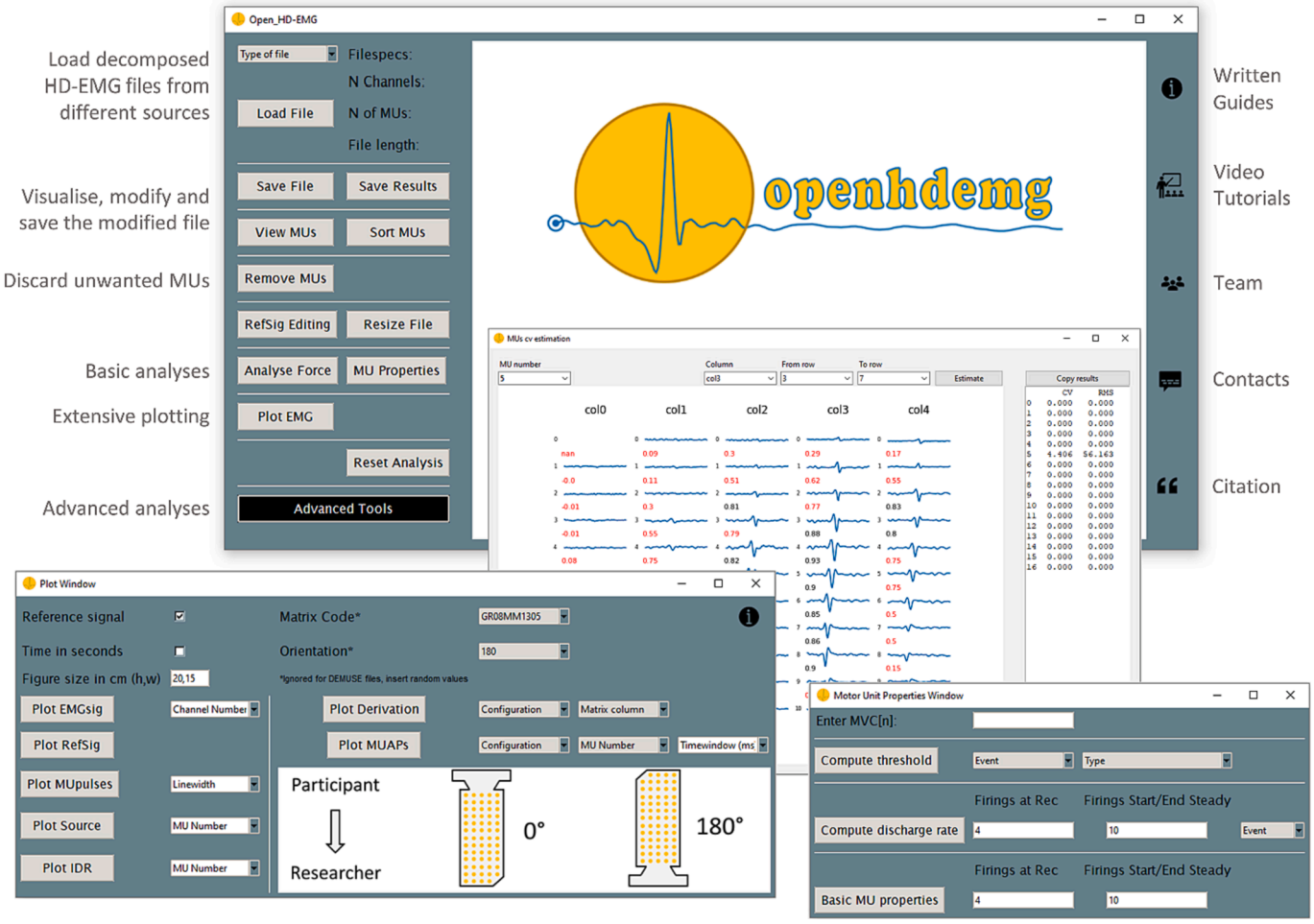

Fig. 2. The Graphical user interface. The *openhdemg* framework is equipped with a practical and functional graphical interface that integrates the most relevant high-level functions of the *openhdemg* library and that allows users to perform a broad range of visualisation, processing and analysis tasks in a time-efficient manner and without coding. High-Density Electromyography, HD-EMG; Motor units, MUs.

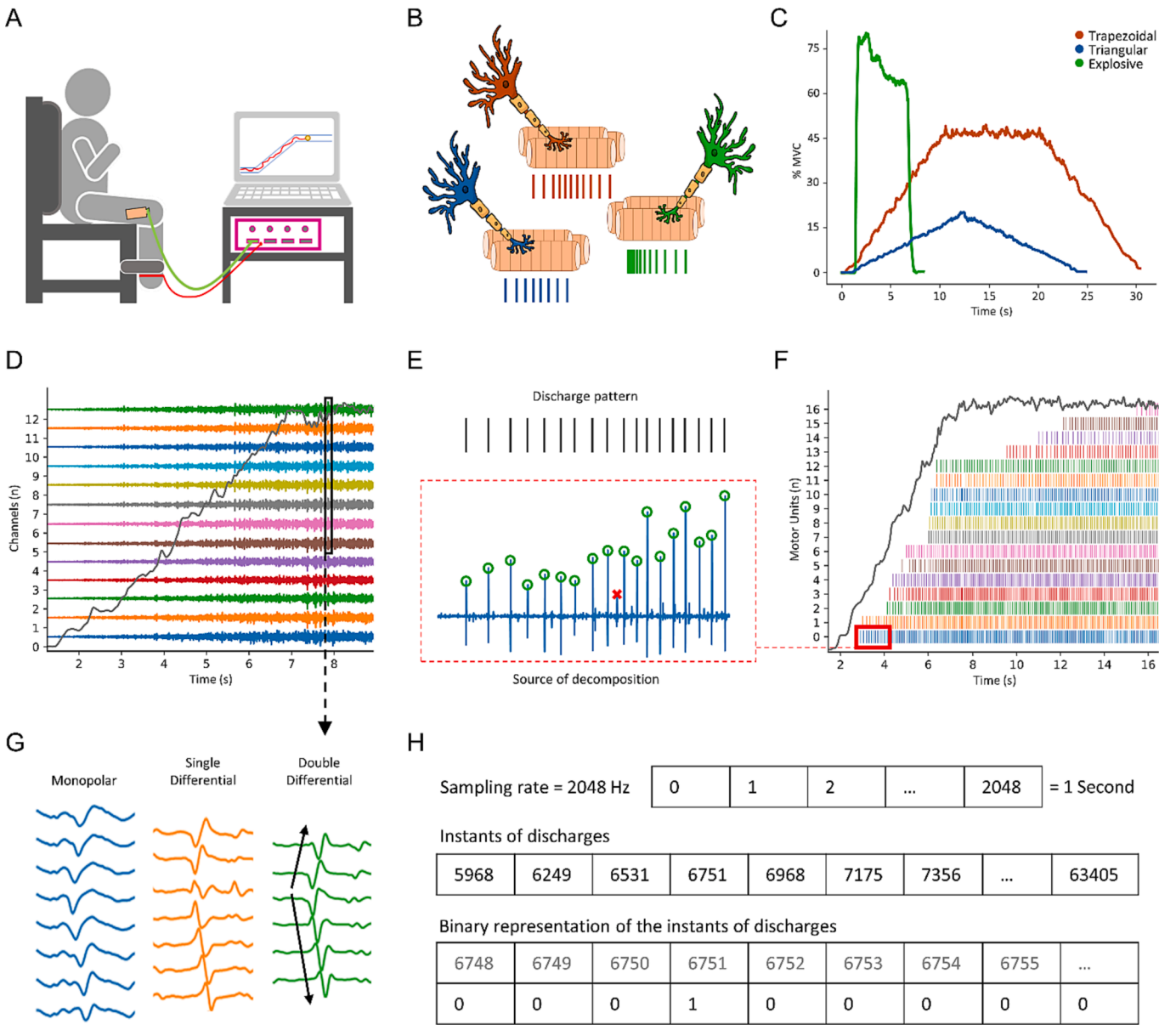

Fig. 3. High-Density surface Electromyography (HD-sEMG) signal acquisition and decomposition. Representative example of HD-sEMG recordings performed during isometric and standardised contractions (A). Specific pools of motoneurons are recruited depending on the target task, resulting in a series of precisely modulated action potentials (B) that cause the depolarisation of the sarcolemma and the generation of the desired muscle force. (C). The summation of all the action potentials generated by different motoneurons generates the interference EMG signal (D) which, if acquired during isometric tasks, can be decomposed in the discharge pattern of individual motor units (MUs) (E, F). For flexibility in the off-line analysis, the interference EMG signal is usually recorded in monopolar montage, although other spatial filtering techniques can be adopted (G). Regardless of the contraction type and setup for EMG signal acquisition, the decomposed HD-sEMG file should contain all the variables necessary for the subsequent analysis of central and peripheral MUs properties, including at least the times of discharge of each MU (H), the raw EMG signal, the auxiliary input signal, the sampling rate, and ideally the decomposed source (E). Maximum voluntary contraction, MVC; number, N; Hertz, Hz.

For the investigation of peripheral MUs properties such as MUs conduction velocity (MUCV) or amplitude of the MUAPs, it is absolutely necessary to standardise the location in which the grid is attached and its orientation (Merletti and Muceli, 2019). Indeed, the estimation of peripheral MUs properties is affected by the dimension and direction of muscle fibres, which vary across the muscle area (Casolo et al., 2023). For these analysis, the grid should be placed following the muscle fibres anatomical orientation and its position should be standardised with respect to an easily-identifiable superficial innervation zone (Martinez-Valdes et al., 2023). Both the direction of the fibres and the innervation zones can be accurately identified with different methods, including the use of linear electrode arrays (Casolo et al., 2020; Del Vecchio et al., 2017) or with low-intensity percutaneous electrical stimulations (Botter et al., 2011) coupled with ultrasound imaging (Hug et al., 2021; Valli et al., 2023).

3.2. Signal decomposition

MUs decomposition is a semi-automated process aimed at extracting the discharge pattern of single MUs from interference EMG signals. Over the last 20 years, different decomposition techniques have been specifically implemented for HD-EMG recordings (Chen and Zhou, 2016; De Luca et al., 2015; Holobar and Zazula, 2007; Nawab et al., 2010; Negro et al., 2016; Ning et al., 2015). These techniques greatly differ in the mathematical approaches employed to discriminate the discharge activity of single MUs, but all provide the same fundamental outcome: the

discharge times of single MUs.

Some of these techniques are considered "automated" because they provide a ready-to-use decomposition outcome (De Luca et al., 2015; Nawab et al., 2010). On the other hand, other approaches such as those based on convolutive blind source separation (Holobar and Zazula, 2007; Negro et al., 2016) are considered "semi-automated". In semi-automated methods, an initial automated phase aimed at identifying and refining the mathematical vectors representing the contribution of single MUs is followed by a manual refinement of the decomposition outcome (as briefly showed in Fig. 3D–F) (Del Vecchio et al., 2020; Enoka, 2019).

While technicalities of MUs decomposition are beyond the scope of this tutorial, it is essential to comprehend the output it generates, which contains the foundational variables for all subsequent analyses on single MUs.

The basic and most important output variable is the time at which each MU is active (Fig. 3F). The times of discharge of each MU are usually represented as a one-dimensional array containing the instants of discharges or, alternatively, as a binary representation of the MUs behaviour over time (i.e., each sample is assigned 0 if the MU is not discharging or 1 if the MU is discharging) (Fig. 3H). This very basic information is fundamental to perform the majority of the analysis, including MUs recruitment and derecruitment threshold (RT and DERT), discharge rate (DR) and MUCV.

In order to estimate the RT and DERT, the information about the times of discharge has to be associated with an auxiliary input signal. Similarly, for the estimation of MUCV or other peripheral properties, the times of discharge have to be associated with the raw multichannel EMG signal. Therefore, these variables have to be included in the decomposed EMG file when the researcher wants to investigate both central and peripheral MUs properties.

Finally, the decomposed file must contain information about the sampling rate, which is fundamental to express all the estimated parameters in time units.

The beforementioned variables in the decomposed HD-sEMG file are sufficient to perform a complete investigation of central and peripheral MUs properties. However, it must be noted that the times of discharge provide very limited information on the reliability of the identified MUs and do not allow to apply any signal-based metrics of accuracy, therefore preventing the discrimination of a properly identified MU from decomposition errors. To overcome this limitation, the files decomposed via blind-source separation contain also the decomposed source, which is the result of the decomposition from which the times of discharge are detected and manually edited, and which allows to estimate the relative magnitude of the spikes in respect to the baseline noise (Holobar et al., 2014; Negro et al., 2016). Conversely, automated techniques such as High-yield decomposition do not contain the decomposed source and estimate decomposition accuracy via, often proprietary, reconstruct-and-test procedures (Nawab et al., 2010).

4. Load the decomposed HD-sEMG file in a working environment

The analysis of the decomposed HD-sEMG files requires specific algorithms or software, which are typically implemented in programming languages such as Python and MATLAB. Therefore, the decomposed HD-sEMG file needs to be imported into a suitable working environment. Since this tutorial is based on *openhdemg*, the only user-friendly solution currently available for the analysis of single MUs activity, the proposed working environment has been specifically designed to enhance the user experience with this framework.

A working environment generally refers to the set of resources necessary to carry out a particular task or job. In the context of this tutorial, we refer to the combination of a computer, a programming language, an integrated development environment and a set of algorithms.

The programming language required by *openhdemg* is Python (v3.11), which can be downloaded and installed from (https://www.python.org/). The integrated development environment is a software that facilitates to write, test, and debug code. The suggested integrated development environment to follow this tutorial is Visual Studio Code (can be downloaded and installed from https://code.visualstudio.com/). Once Python and Visual Studio Code are installed, the user needs to download the set of pre-built algorithms (usually named "library" in Python, which indicates a collection of reusable code modules and functions). As previously mentioned, *openhdemg* is the library used in this tutorial. *openhdemg* is hosted at PyPI (https://pypi.org/project/openhdemg/) and can be installed as "pip install openhdemg" from the Python terminal. The user is encouraged to install openhdemg and other libraries in a specific "virtual environment", which is a self-contained directory that contains a specific version of Python and its dependencies. The users without previous experience using Python are strongly encouraged to follow the detailed guide through the beforementioned steps at (https://www.giacomovalli.com/openhdemg/tutorials/setup_working_env/).

Once the working environment is set, the user is ready to perform the analyses presented in this tutorial exploiting the functionalities of *openhdemg*. As previously introduced, the code necessary to analyse the decomposed HD-sEMG file will not be presented in the main text of the manuscript, which will instead prioritise the theoretical and visual aspects. However, the user can download different Python files (.py extension) that contain all the code necessary to replicate the analyses presented in this tutorial alongside an extensive step-by-step explanation of the code provided. These files can be opened and executed directly in Visual Studio Code.

The user that immediately wants to test the example code can download 4 decomposed example files (named Pre_25_a, Pre_25_b, Post_25_a and Post_25_b). The recordings have been performed 4 weeks apart (i.e., "Pre" and "Post") in a young subject performing moderate physical activity. For each timepoint, the same muscle contraction was performed twice, and distinguished by the labels "a" and "b.". These sample files contain all the variables necessary to investigate both central and peripheral MUs properties. Both the example scripts and the example decomposed files can be downloaded from https://www.giacomovalli.com/openhdemg/isek_jek_tutorials/ or from https://data.mendeley.com/datasets/g2p2r6b5zr/1.

For the scope of this tutorial, we are using example files decomposed via blind source separation (Negro et al., 2016), as these will allow us to present also signal-based metrics of accuracy. However, files from any recording system or decomposition technique could be utilized, as *openhdemg* offers various functions for loading different decomposition outcomes into a standardized data structure. This common data structure is essential to ensure that the same set of functions can be applied uniformly to process different sources, regardless of their original format.

5. Visualization, inspection and processing of decomposition outcome

As shown in Fig. 4A, the sample decomposed HD-sEMG file contains a trapezoidal contraction ranging from 0 to 25 % MVC for a total duration of about 30 s. In this example file, the auxiliary input signal represents the participant's generated force and is expressed as % MVC. This type of contraction is very common in HD-sEMG studies and it has been preferred for the scope of the tutorial as it allows to detect the progressive and ordered recruitment and derecruitment of different MUs and their DR modulation during voluntary isometric contractions (Nuccio et al., 2021; Valli et al., 2023).

As research in HD-sEMG advances, however, different types of contraction such as triangular and explosive contractions, are also becoming of common use to address specific research questions (Del Vecchio et al., 2019b; Hassan et al., 2021; Mesquita et al., 2022).

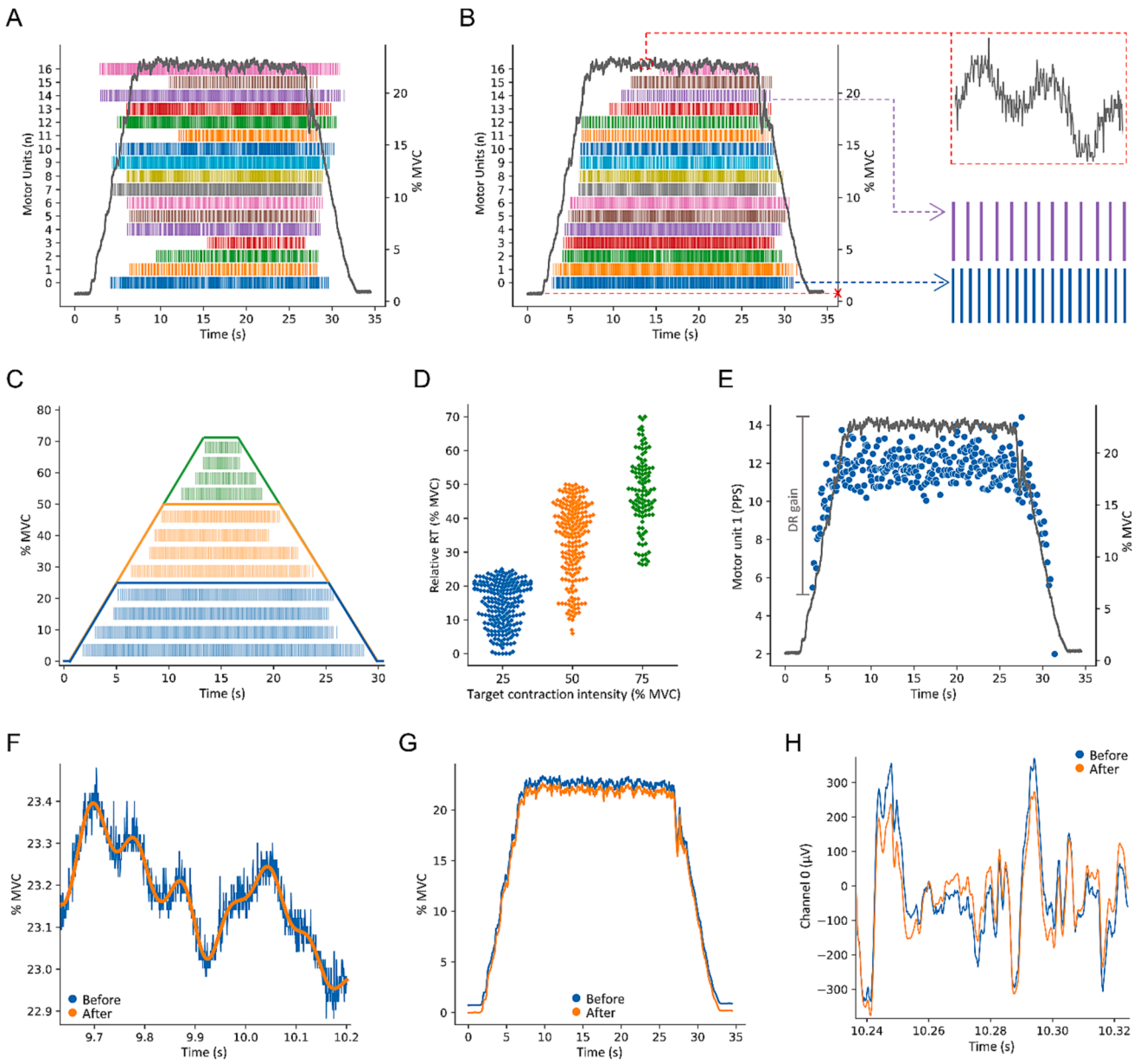

Fig. 4. Visualization, inspection and processing of decomposition outcome. The content of the decomposed High-Density surface Electromyography (HD-sEMG) file can be practically inspected by visualising the binary representation of motor units (MUs) discharge times eventually coupled with the auxiliary input signal (A). To better detect the distribution of the decomposed MUs, these can be visualised based on their order of recruitment (B). In this visualisation, the recruitment thresholds provide information on whether the decomposition procedure identified MUs through the majority of the volitional recruitment range of the tested muscle, or only at specific force levels, as typically observed in contractions executed at higher force levels (C, D). The discharge behaviour of single MUs can be better visualised by the instantaneous discharge rate which, in the showed example, reflects the motoneuron's linear response to the depolarizing current it receives (E). The auxiliary input signal can be adjusted before the analysis via filtering of the noisy components (F) (in this example figure, a 4th order, zero-lag low-pass Butterworth filter with 15 Hz cut-off frequency was used) and via removal of signal offset (G). Similarly, also the EMG signal can be filtered if the decomposed HD-sEMG file only contains its unprocessed version (H) (in this example figure, a 2nd order, zero-lag band-pass Butterworth filter with a frequency range of 20–500 Hz was used). Maximum voluntary contraction, MVC; number, N; recruitment threshold, RT; pulses per second, PPS.

Obviously, the flexibility and customisability of the *openhdemg* framework makes it suitable also to work with these (and other) novel contraction types.

In Fig. 4B, the same MUs have been sorted based on their order of recruitment. This visualisation is useful to detect the distribution of the decomposed MUs and whether the decomposition procedure identified MUs through the whole or the majority of the volitional recruitment range of the tested muscle, or only at specific force levels. The latter phenomenon can be typically observed in contractions executed at higher force levels (e.g., 50 or 70 % MVC) where the superimposition of larger MUAPs generated by MUs with higher RT might prevent the observation of the smaller MUAPs generated by lower-threshold MUs (Fig. 4C–D) (Casolo et al., 2021; Del Vecchio et al., 2019a; Valli et al., 2023).

From the visualisation of the discharge times, however, it is difficult to have a complete understanding of the MUs discharge activity. Therefore, it is usually more informative to visualise each MUs discharge pattern both as a function of time (X axis, in seconds) and as a function of DR (left Y axis, in pulses per second) as shown in Fig. 4E. Indeed, from this representation of the MUs discharge activity, it is possible to observe some typical physiological characteristics of the MUs discharge such as the motoneuron's linear response to the depolarizing current it receives

(Fig. 4E) (Mendell, 2005) and the common drive to the muscle (Fig. 4B) (De Luca and Erim, 1994).

Regarding muscle force, Fig. 4B highlights two common problems in HD-sEMG recordings: (i) the auxiliary input signal shows the presence of a signal offset and (ii) of a noisy component that might affect some analyses like the MUs RT and DERT.

The beforementioned examples and observations, although do not provide any objective measurement, present a clear overview of the quality of the HD-sEMG recording and decomposition output, and grant enough guidance for editing the HD-sEMG file before estimating the MUs properties.

In this regard, the *openhdemg* library offers a complete pipeline for the processing of the decomposition outcome before MUs analysis, including the removal of auxiliary input signal offset and different filtering techniques to reduce electric noise, both in the auxiliary input and in the raw EMG signal when needed (as exhaustively shown in the code implementation and in Fig. 4F–H).

In the context of this tutorial article, we recognize the need to explicitly state that signal filtering is a complex topic and that the appropriate filter type should be selected based on the user's specific needs. We therefore redirect the reader to more specific articles covering this topic (Clancy et al., 2002; McManus et al., 2020).

A final adjustment, often necessary while preparing the HD-sEMG file for analyses, is to remove areas of the recording with unwanted neuromuscular activation before and after the actual contraction phase (e.g., movement artefacts). This editing can be efficiently performed by resizing the HD-sEMG file in a narrower time-window that only includes the active contraction phase. During this process, the user should be

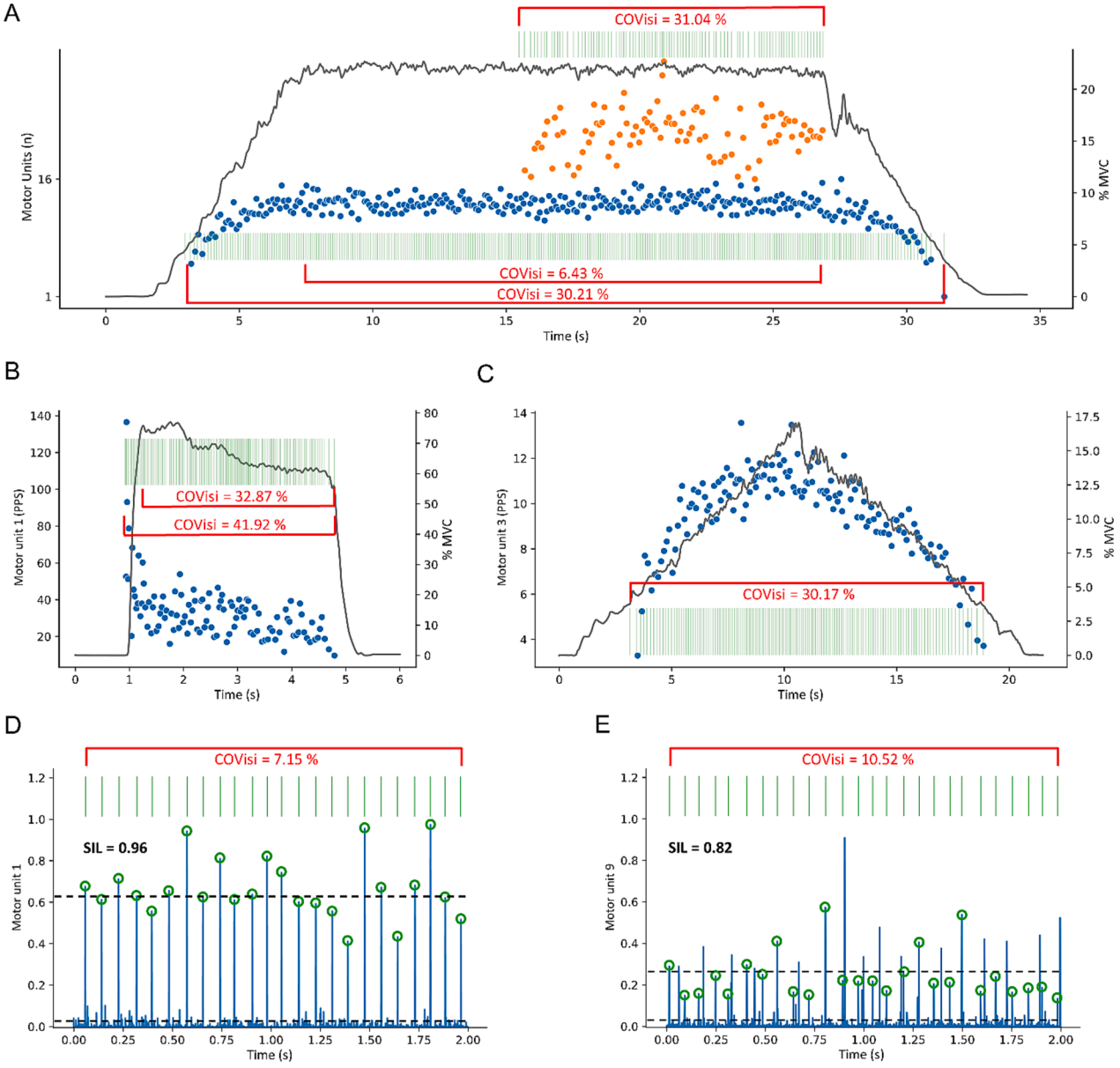

Fig. 5. Accuracy of the identified motor units. The coefficient of variation of interspike interval (COVisi) estimates the regularity of the motor units (MUs) discharge events. When applied to the steady-state phase of trapezoidal contractions, it can be used to estimate the accuracy of the identified MU (e.g., MU 1 vs MU 16 in panel A). However, the COVisi is greatly affected by the discharge rate (DR) modulation necessary to increase or decrease muscle force production. Indeed, the COVisi is not an appropriate metric for contractions with a very short (B) or completely absent (C) steady-state phase. The silhouette score (SIL) is a signal-based metrics of accuracy estimating the separation between the signal (the source signal at the time of firing of the identified MU) and the noise. The SIL is therefore estimated on the decomposed source and is not affected by the discharge behaviour of the MU. Additionally, being a normalised value, it provides a clear indication of correctly (D) and incorrectly (E) identified MUs. Maximum voluntary contraction, MVC; pulses per second, PPS.

careful to resize the EMG and auxiliary input signal in the same time window but, at the same time, all the other variables in the time domain, or depending from the time-window of interest, should be adjusted accordingly. For example, If the EMG signal is resized, all the instants of discharge will take a different value, which can be simplified as the original value minus the number of samples removed from the initial part of the HD-sEMG file.

6. Discard unwanted MUs based on objective criteria

The term "unwanted MUs" is used to indicate those MUs that do not respect some qualitative criteria of accuracy or with irrelevant features for the intended analysis. In the context of HD-sEMG and MUs detection, the term" accuracy" refers to the accurate identification of the MUs discharge behaviour with respect to their physiological discharge pattern, which can be either known a priori in simulation studies or assumed from intramuscular recordings (Holobar et al., 2009; Mambrito and De Luca, 1984).

One of the reasons why MUs activity is usually investigated during standardised tasks is that the discharge behaviour of the MUs is highly predictable from the performed task. Consequently, unexpected and unregular discharge profiles might indicate errors in the identification of the specific MU discharge times, at least in healthy individuals.

For example, during trapezoidal contractions, the frequency of the discharge pattern of each MUs is expected to progressively increase from the moment of recruitment through all the ascending phase of the contraction. Similarly, the steady-state phase should show a maintenance of the frequency (or a slow and constant decrease) that is then progressively reduced during the descending phase (Fig. 5A) (Del Vecchio et al., 2017; Pascoe et al., 2014).

In light of this, a common parameter used to estimate the physiological behaviour of the identified MUs (and to indirectly infer on their accuracy) is the variability of the MUs discharge pattern during the steady-state phase of the contraction (Hu et al., 2014). This variability can be estimated as the coefficient of variation of the interspike interval (COVisi), which is the ratio between the standard deviation of the interspike interval (ISI) array and its average value, usually expressed in percent. The ISI array represents the time-difference between consecutive discharge instants of each MU.

High values of the COVisi indicate high variability in the MUs discharge pattern and, according to recent consensus and research articles, the COVisi during the steady-state phase of the contraction could serve as a criterion for identifying inaccurate MUs and excluding them from subsequent analyses (Gallina et al., 2022; Martinez-Valdes et al., 2017).

However, there are limitations in the use of the COVisi as a criterion to determine the reliability of the decomposition. Indeed, the type of contraction heavily influences the MUs ISI and its variability, which might be elevated also in accurately identified MUs whenever the steady-state phase is either very short (2–5 s) or completely absent (as showed in Fig. 5B–C). Additionally, MUs behaviour in non-physiological conditions such as neuromuscular diseases and extreme muscle fatigue might not respect the assumption of regular discharge activity of the MUs, therefore preventing the use of COVisi as a metric to evaluate the accuracy of the decomposition (Holobar et al., 2012; Taylor et al., 2016).

Another approach for the discrimination of accurately identified MUs consists in the use of signal-based metrics of accuracy such as the pulse to noise ratio (PNR) (Holobar et al., 2014) or the silhouette score (SIL) (Negro et al., 2016), which are estimated from the decomposed source.

The PNR is a ratio between the signal and the noise (i.e., the time moments in which the MU is estimated to have or not to have discharged) expressed in decibels (dB). Specifically, the distinction between signal and noise is determined by a threshold estimated via a heuristic penalty function that accounts for the variability of the ISI and for the MUs DR (Holobar et al., 2012). Therefore, also the PNR value is influenced by the MUs discharge behaviour (Holobar et al., 2014). Common PNR thresholds used to determine a sufficient level of accuracy are PNR $\geq$ 30 dB, although also PNR $\geq$ 28 dB could be accepted if supported by a careful visual inspection of the MUs discharges by experienced investigators (Holobar et al., 2014; Valli et al., 2023).

The SIL provides an estimation of reliability similar to the PNR although with a different approach. Indeed, the SIL is defined as the normalized measure of the distance between the clusters of the detected discharge points and the cluster of the noise values (Fig. 5D and 5E). Compared to the PNR, the SIL has two main advantages in the estimation of accuracy as (i) it does not depend on the discharge behaviour of the MUs and (ii) being a normalised measure ranging from 0 to 1, it is of easy interpretation and directly associated to metrics like the rate of agreement that are commonly used in the validation of the decomposition algorithms (Negro et al., 2016).

Common SIL thresholds used to determine a sufficient level of accuracy are SIL $\geq$ 0.9. However, as for the PNR, lower values of about 0.88 can be accepted if supported by careful visual inspection of the MUs discharges by experienced investigators (Negro et al., 2016).

7. Track MUs within and between recording sessions

The possibility to recognise and track the same MU across different recordings and recording sessions opened new possibilities in the understanding of how MUs adjust to various types of interventions, including muscle disuse and pharmacological treatments (Goodlich et al., 2023; Valli et al., 2023). Indeed, comparing the same population of MUs over time provides a more robust estimation of their changes and filters the contribution of different MUs that can be detected at different data collection points (Maathuis et al., 2008; Martinez-Valdes et al., 2017).

The recognition of the same MU is based on the comparison of their MUAPs representation across the channels of the recording grid, thus accounting both for the shape of the MUAPs and their spatial distribution. The estimation of the MUAPs is accomplished via spike-triggered averaging of the EMG signal (Stein et al., 1972; Taylor et al., 2002). Spike-triggered averaging involves identifying a specific time window (e.g., 50 ms) in the EMG signal centred on each firing event of a MU, and then averaging all the signals within that window. This procedure, that has to be performed in each grid channel, enhances the definition of the MUAP by reducing the contribution of action potentials generated by neighbouring MUs. A visual representation of the spike-triggered averaging technique is provided in Fig. 6A.

For MUs tracking, the spike-triggered averaging is often performed on the single differential derivation of the EMG signal, because the comparison of the MUAPs in monopolar configuration tends to overestimate similarities (Martinez-Valdes et al., 2017). The single differential signal is calculated by subtracting the EMG signal in two adjacent channels of the grid along the direction of the muscle fibres.

The estimation of similarity between the MUAPs representation of two MUs is usually achieved via two-dimensional cross-correlation analysis (Martinez-Valdes et al., 2017). This analysis returns a two-dimensional array of values representing a subset of the discrete linear cross-correlation between the input that is then normalised for the different energy levels of the two MUs. The cross-correlation coefficient (XCC) is computed as the maximum value of the normalised cross-correlation array. XCC represents the degree of correlation between the two arrays, with values closer to 1 indicating a stronger correlation. In cases where a MU exhibits high correlation with multiple MUs in the other contraction, only the MU with the highest XCC is considered for the pair matching (Martinez-Valdes et al., 2017).

The tracking technique maximises the likelihood of observing the same MU in different recordings and proved to be effective also after weeks of various interventions (Casolo et al., 2020; Del Vecchio et al., 2019a; Martinez-Valdes et al., 2018; Valli et al., 2023). It should be

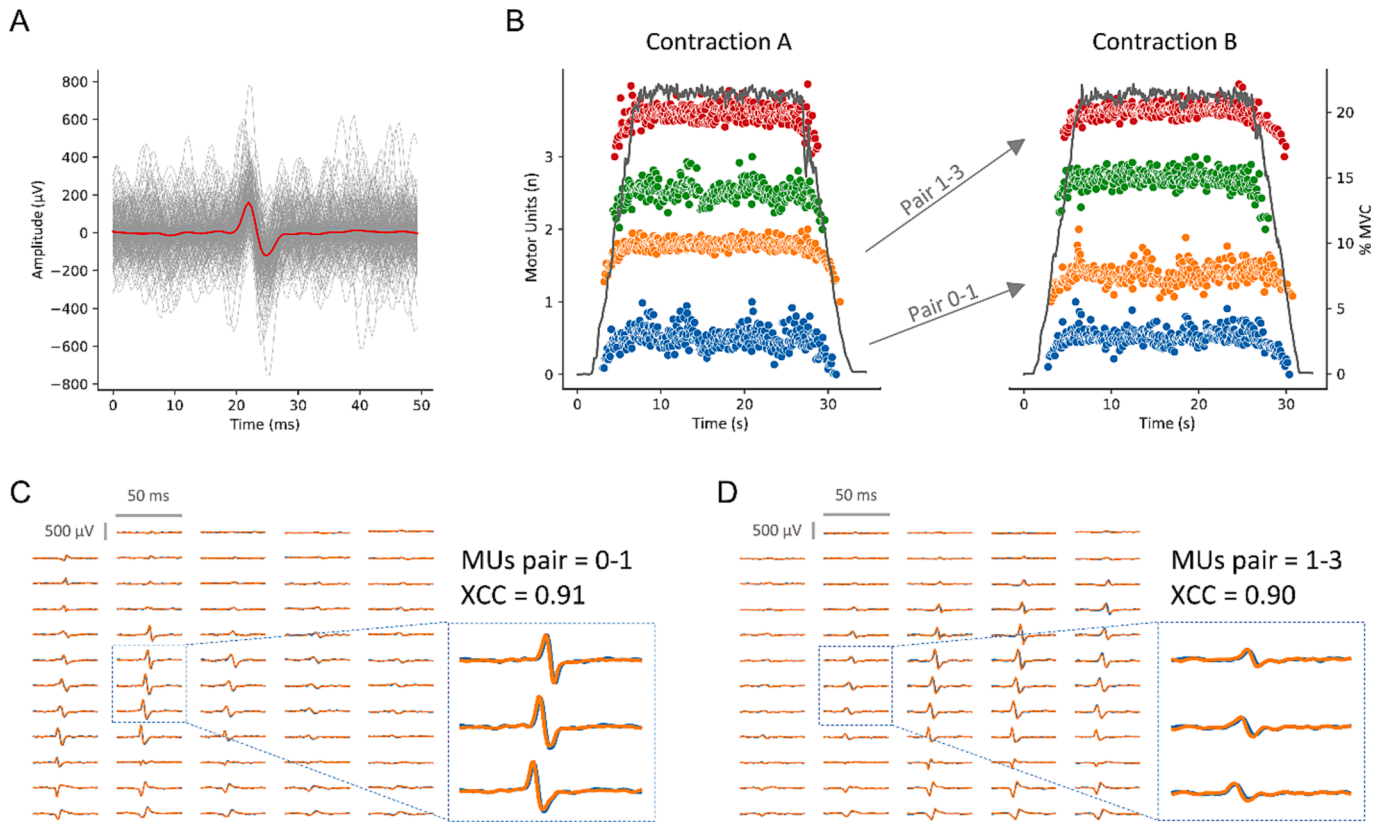

Fig. 6. Motor units tracking. The shape and spatial representation of motor units (MUs) action potentials (MUAPs) shape allows for the recognition of the same MU within and between recording sessions. The estimation of smooth MUAPs is performed via averaging of all the MUAPs representations at each discharge event of the investigated MU (A). The tracking procedure is performed via two-dimensional cross-correlation analysis of the MUAPs representation (B, C, D). In these example figures, the MUAPs have been estimated from the single differential spatial filtering. The visualisation of the overlapping MUAPs of tracked pairs is fundamental for the validation of the cross-correlation analysis and must be always performed, regardless of the cross-correlation coefficient (XCC) valueb (C, D). Number, N; maximum voluntary contraction, MVC.

noted, however, that a number of factors can undermine the successful tracking. When the tracking is performed in different recording sessions, the grid of electrodes has to be re-applied at each data collection point and changes in the grid position will alter the MUAPs representation over the different electrodes. Therefore, it is fundamental to re-apply the grid in the same exact position at each recording session. To date, the most precise way to ensure correct placement consists in marking the skin with a permanent marker. Apart from technical aspects, muscle morphology and MUAPs can also be affected by particular interventions (Inns et al., 2022; Sarto et al., 2022b), thus requiring extra attention in the validation of the tracking results.

Due to the possible confounding factors in the longitudinal MUs tracking, it becomes of extreme importance to check the reliability of the cross-correlation measure by visualising the overlying MUAPs from the pair of MUs across each channel, and to determine the inclusion/exclusion by verifying the effective overlapping of the MUAPs shape and their spatial distribution (Fig. 6B–D).

In order to account for the minor differences in grid placement or changes in the MUAPs profile, the XCC threshold is commonly set ≥ 0.8 (Cudicio et al., 2022; Lulic-Kuryllo et al., 2021; Oliveira and Negro, 2021), although some authors adopted also XCC ≥ 0.7 (Casolo et al., 2020; Del Vecchio et al., 2019a).

After identifying pairs of MUs, the user can decide to perform the subsequent statistical analyses considering both the populations of total and tracked MUs. In this case, the tracked population can be used as a validation of the results observed in the total population (Valli et al., 2023). Alternatively, if the tracked population of MUs is sufficiently large and representative, the analysis can be exclusively performed on the tracked MUs. This elegant approach allows for the precise detection of single MU changes over time, offering valuable insights into the dynamics and adaptations of the neuromuscular system (Casolo et al., 2020).

Recently, MUs tracking has also been employed for the identification of the same MUs within the same recording session (Valli et al., 2023) with an XCC threshold ≥ 0.9 because this condition doesn't need to account for a different placement of the recording grid or for changes in MUAPs due to interventions, as previously proposed (Maathuis et al., 2008).

8. Analyse central MUs properties

Sections 8 and 9 will introduce a number of fundamental parameters for the analysis of MUs properties that are often tuned based on empirical observations, personal experience and experimental needs. Therefore, the proposed values should only be considered as representative examples that do not constitute standards. Indeed, this necessity of flexibility is embraced by the *openhdemg* framework, which allows the user to fully customise any implemented function based on specific needs (as demonstrated in the code implementation).

The definitions of the various properties presented in section 8 and 9 are based on recent consensus statements. For more comprehensive explanations, readers are directed to (Gallina et al., 2022; Martinez-Valdes et al., 2023; McManus et al., 2021).

MUs RT/DERT and DR are often referred as "central" properties due to their close relation with the discharge behaviour of the innervating motoneurons (Heckman and Enoka, 2004). Indeed, these variables reflect the intrinsic properties of each motoneuron and the integrated modulatory stimuli it receives, making them of primary interest in the

study and characterisation of the neural control of voluntary muscle force production (Heckman and Enoka, 2012).

MU RT and DERT are simply defined as the force level at which a motor unit begins and ends to discharge action potentials repetitively. Therefore, for the analysis of MUs RT and DERT, the presence of an auxiliary input signal representing the participant's muscle force is fundamental. The auxiliary input signal can be expressed in different units of measurement (e.g., V, mV, Kg, N, Nm) and it is often reported in both absolute and normalised terms (i.e., as % MVC).

In practical terms, the estimation of these two parameters can be simply performed by identifying the first and last element in the array containing the times of discharge of each MU, and then extracting the value for the auxiliary input signal at the corresponding instants (Fig. 7A).

MUs DR is defined as the number of action potentials discharged per second by a single MU. However, given its variability during contractile tasks, it is common practice to visualise the instantaneous DR, which is obtained dividing the sampling rate by the ISI between two consecutive discharges (Fig. 7A). Of note, MUs DR is expressed as pulses per second (PPS), unlike typical frequency units.

In order to reduce this variability and to obtain a more robust estimation, MUs DR is usually analysed and reported as the average instantaneous DR over a number of consecutive discharges. MUs DR can

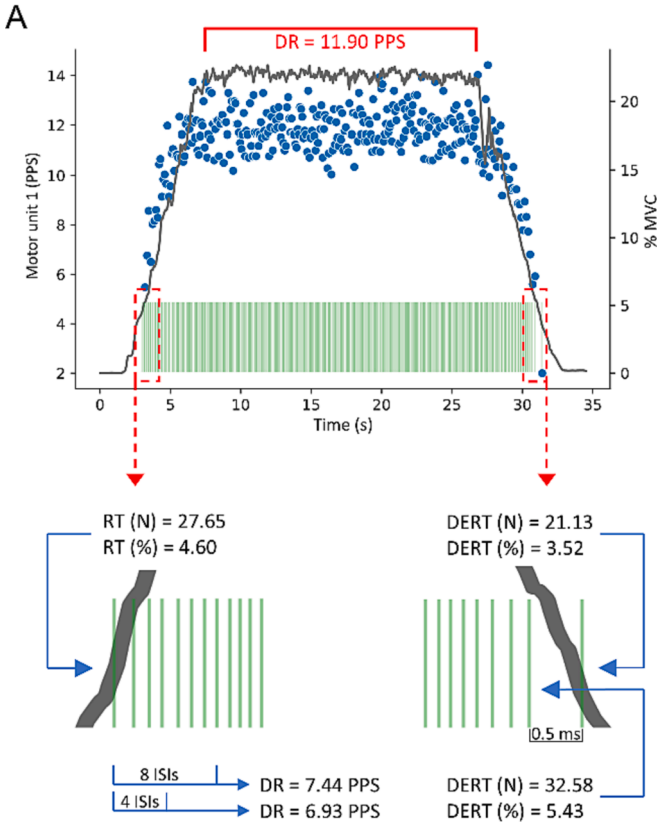

Fig. 7. Analysis of central motor units properties. Motor units (MUs) recruitment threshold (RT) and derecruitment threshold (DERT) are estimated as the force value (which can be expressed both in absolute and relative terms) at which the MU begins or stops to discharge action potentials repetitively. In this example, MUs discharge rate (DR) is estimated as the average value of a number of consecutive discharges at recruitment, derecruitment and during the entire steady-state phase. Based on the criteria used to manually determine the inclusion and exclusion of firings, the results of these analyses can vary significantly. Therefore, it is necessary to consistently adopt the same criteria for the manual editing of MUs discharges in order to have consistent and reliable results from the analysis of central MUs properties. Pulses per second, PPS; maximum voluntary contraction, MVC; interspike intervals, ISIs.

be estimated within different phases of a voluntary contraction, such as in the recruitment phase, derecruitment phase and the steady-state phase. For recruitment and derecruitment, it is necessary to find a compromise between robustness and sensitivity (Del Vecchio et al., 2020). This is often achieved by averaging the intervals generated by few (e.g., 3–5) consecutive discharges at the beginning and at the end of the contraction (Fig. 7A) (Del Vecchio et al., 2019a; Valli et al., 2023). During the steady-state phase, all firings can be averaged (Škarabot et al., 2023). However, if the steady-state phase is long (e.g., > 20–25 s), the estimation of MUs DR is affected by the physiological decline in DR, especially for MUs with lower recruitment thresholds (Pascoe et al., 2014). In such cases, it is possible to limit the estimation of MUs DR to a fixed number of discharges (e.g., 20–50) at the beginning of the steady-state phase.

9. Analyse peripheral MUs properties

MUCV and amplitude of the action potentials are often referred to as "peripheral" properties, as they primarily depend on the morphology and biology of the innerved muscle fibres (Casolo et al., 2023). Therefore, these two parameters have significant physiological relevance in the investigation of aspects concerning the generation and propagation of the MUAPs in response to the motoneuron discharges (Blijham et al., 2006; Campanini et al., 2009).

MUCV represents the speed at which the MUAPs propagate along the sarcolemma of the muscle fibres belonging to single MUs and it is considered a "size principle parameter" due to its linear association with MUs RT and with muscle fibre diameter (Andreassen and Arendt-Nielsen, 1987; Casolo et al., 2023; Del Vecchio et al., 2017).

MUAP amplitude is considered an important parameter for inferring the size of single MUs, but it must be noticed that estimation from surface HD-sEMG recordings presents high variability. Indeed, MUAP amplitude is considerably influenced by muscle architecture, subcutaneous tissue thickness and proximity of the MU, among other factors. Although this value can be informative, the direct estimation of MUs size from measures of MUAP amplitude is not generally recommended (Martinez-Valdes et al., 2023). MUAP amplitude can be quantified using various measures, including peak-to-peak distance or root-mean-square of the MUAPs. When reported alongside MUCV, MUAP amplitude can be calculate on the same MUAPs and channels used for MUCV estimation (Del Vecchio et al., 2017).

The estimation of the MUAPs for the analysis of peripheral MUs properties is usually performed via spike-triggered averaging of the EMG signal as previously described. For the estimation of MUCV, the spike-triggered averaging is usually computed on the double differential derivation of the EMG signal along the direction of the muscle fibres. This spatial filtering decreases the presence of non-propagating components and attenuates the end-of-fibre effect, thus enhancing the representation of MUAPs propagation (Fig. 8A–C) (Gallina et al., 2022). The double differential signal is calculated over three adjacent channels of the grid by subtracting the EMG signal in the first channel from twice the EMG signal in the second channel, and then subtracting the EMG signal in the third channel.

Given the definition of MUCV as a size principle parameter, the spike triggered average for this analysis is usually calculated over a number of discharges that provide a balance between the smoothing in the MUAPs (improved by a higher number of averaged samples) and the representation of the MUCV value at the recruitment phase. Although there is no reference value, the actual literature seems to favour the computation of the spike-triggered average over the first 20–50 discharges at recruitment (Casolo et al., 2023; Martinez-Valdes et al., 2018).

On the generated MUAPs, the estimation of MUCV is performed via maximum likelihood estimation of the time delay over a number of channels with specific characteristics. Given its complexity, the technical implementation of the maximum likelihood estimation cannot be explained adequately in this tutorial and the reader is encouraged to

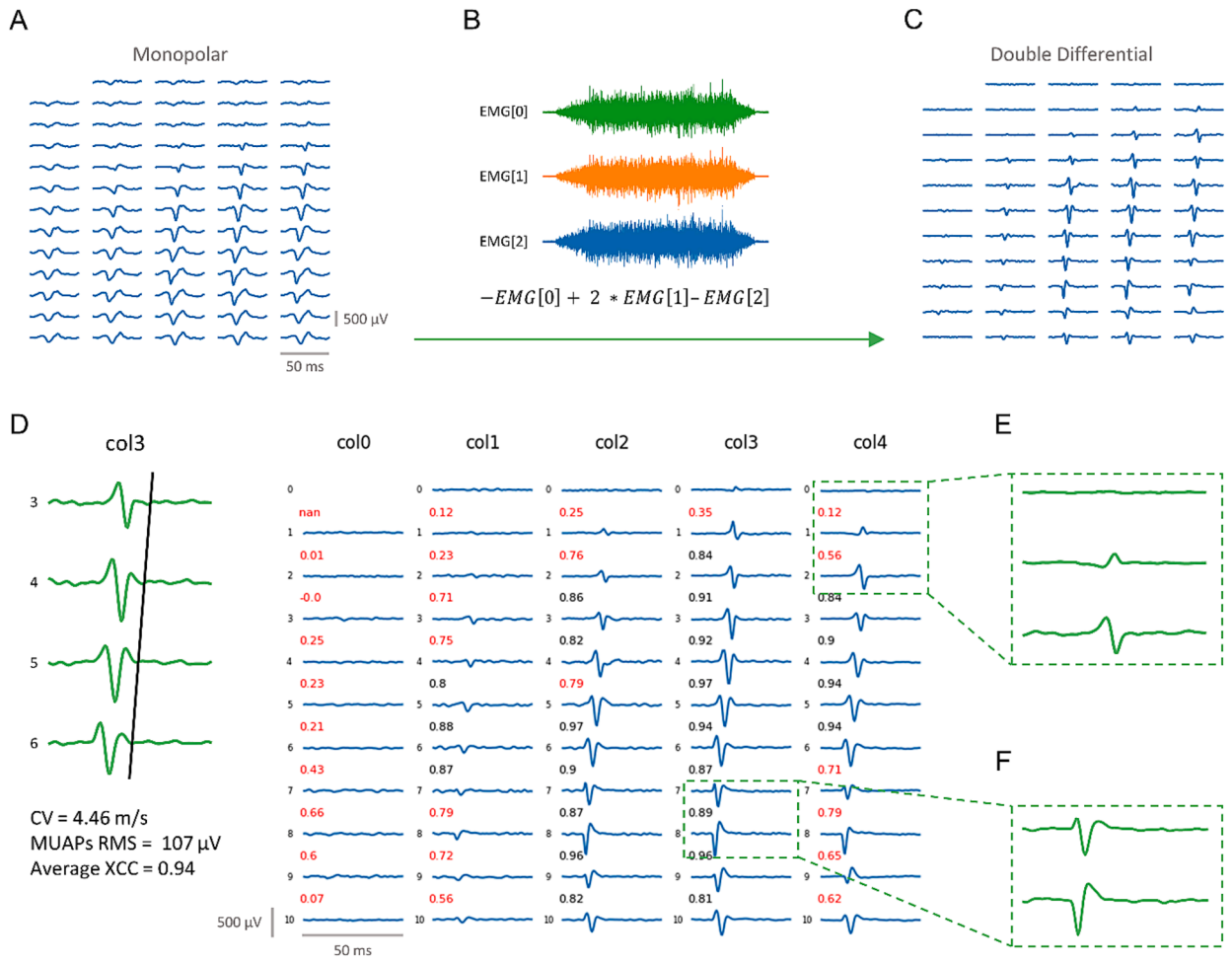

Fig. 8. Analysis of peripheral motor units properties. The estimation of motor units (MUs) conduction velocity (MUCV) is usually performed on the MUs action potentials (MUAPs) representation estimated from the double differential spatial filtering of the raw EMG signal (A, B, C). MUCV represents the speed at which the MUAPS propagate along the sarcolemma of the muscle fibres (D). For the reliable estimation of MUCV, it is fundamental to select the largest number of adjacent channels (in the direction of muscle fibres, represented in columns in the *openhdemg* interface) showing a clear propagation of action potentials and high cross-correlation coefficients (XCC). In the selection of the channels, it is necessary to avoid the MUAPs presenting the end-of-fibres effect (extinction of action potentials) (E) and the innervation zone (inversion in the propagation direction) (F), as these will significantly alter the estimation of the MUCV value.

read specific articles on the topic (Farina et al., 2002; Farina et al., 2000).

The identification of channels for estimating MUCV involves a manual selection process. It requires the visual examination of adjacent channels within a column of the grid to identify those that show the clearest propagation of the action potential and exclude the innervation zone (identified as the inversion of the action potential shapes and of their direction of propagation). The choice of the channels is supported by the cross-correlation value between adjacent pairs. This cross-correlation analysis helps in identifying pairs with strong similarities in their MUAP patterns, indicating consistent propagation characteristics. Additionally, a minimum cross correlation threshold is often employed to ensure the acceptability of pairs. Similarly to MUs tracking, a threshold ≥ 0.8 is expected to yield most reliable estimations, although a cross-correlation threshold ≥ 0.7 is also often adopted (Škarabot et al., 2023). A minimum of 2 channels are technically sufficient for MUCV estimation via maximum likelihood. However, it is strongly recommended to include 3 or more channels to increase the accuracy of the estimates.

It is important to note that the physiological range of MUCV during voluntary contractions typically falls between 2 and 8 m/s (Beretta-piccoli et al., 2019; Farina et al., 2002). Any values outside of this range are likely to be the result of errors in data collection (e.g. electrodes misalignment) or analysis (e.g., wrong selection of the channels) and should be disregarded or further investigated.

Given the complexity of the selection of appropriate channels, and the necessity of visual inspection, the user is encouraged to refer to Fig. 8D–F for a clear presentation of this procedure.

10. Final remarks and conclusions

This tutorial provides a detailed explanation of crucial steps for the analysis of MUs properties from decomposed HD-sEMG recordings. Furthermore, it introduces the possibility to perform MUs analyses with *openhdemg*, an efficient tool that can lower the barriers to the implementation of the HD-EMG technique thanks to its user-friendly structure, extensive documentation, and flexible architecture easily accessible to researchers with varying levels of programming experience.

openhdemg is an opensource framework in continuous expansion and will continue to evolve based on user feedback and emerging research needs, fostering collaboration and knowledge sharing within the HD-EMG community.

Funding

No funding has been received both for the manuscript and for the development of the *openhdemg* framework.

Author contributions

All the authors approved the final version of the manuscript, agree to be accountable for all aspects of the work in ensuring that questions related to the accuracy or integrity of any part of the work are appropriately investigated and resolved. All persons designated as authors qualify for authorship, and all those who qualify for authorship are listed. GV conceptualised and designed *openhdemg* and the tutorial. GV implemented the functions for electromyography data handling, visualisation, editing and analysis. PR implemented the graphical user interface. FN provided technical support and supervision for the development of the analysis algorithms. AC tested the functions and the graphical user interface and provided guidance for the implementation of missing functionalities. GDV provided overall direction and organisation of the project. GV drafted the manuscript with the support of AC, and all the authors revised it. GV maintains the GitHub and PyPI repositories and supervises the future development of *openhdemg*.

Declaration of competing interest

The authors declare that they have no known competing financial interests or personal relationships that could have appeared to influence the work reported in this paper.

References

Andreassen, S., Arendt-Nielsen, L., 1987. Muscle fibre conduction velocity in motor units of the human anterior tibial muscle: A new size principle parameter. J. Physiol. 391, 561–571. https://doi.org/10.1113/JPHYSIOL.1987.SP016756.

Beretta-piccoli, M., Cescon, C., Barbero, M., Antona, G.D., 2019. Reliability of surface electromyography in estimating muscle fiber conduction velocity : A systematic review. J. Electromyogr. Kinesiol. 48, 53–68. https://doi.org/10.1016/j.jelekin.2019.06.005.

Besomi, M., Hodges, P.W., Dieën, J.V., Carson, R.G., Clancy, E.A., Disselhorst-klug, C., Holobar, A., Hug, F., Kiernan, M.C., Lowery, M., Mcgill, K., Merletti, R., Perreault, E., Søgaard, K., Tucker, K., Besier, T., Enoka, R., Falla, D., Farina, D., Gandevia, S., Rothwell, J.C., Vicenzino, B., Wrigley, T., 2019. Consensus for experimental design in electromyography (CEDE) project : Electrode selection matrix. J. Electromyogr. Kinesiol. 48, 128–144. https://doi.org/10.1016/j.jelekin.2019.07.008.

Blijham, P.J., Ter Laak, H.J., Schelhaas, H.J., Van Engelen, B.G.M., Stegeman, D.F., Zwarts, M.J., 2006. Relation between muscle fiber conduction velocity and fiber size in neuromuscular disorders. J. Appl. Physiol. 100, 1837–1841. https://doi.org/10.1152/JAPPLPHYSIOL.01009.2005.

Botter, A., Oprandi, G., Lanfranco, F., Allasia, S., Maffiuletti, N.A., Minetto, M.A., 2011. Atlas of the muscle motor points for the lower limb: Implications for electrical stimulation procedures and electrode positioning. Eur. J. Appl. Physiol. 111, 2461–2471. https://doi.org/10.1007/s00421-011-2093-y.

Campanini, I., Merlo, A., Farina, D., 2009. Motor unit discharge pattern and conduction velocity in patients with upper motor neuron syndrome. J. Electromyogr. Kinesiol. 19, 22–29. https://doi.org/10.1016/j.jelekin.2007.06.018.

Casolo, A., Farina, D., Falla, D., Bazzucchi, I., Felici, F., Del Vecchio, A., 2020. Strength training increases conduction velocity of high-threshold motor units. Med. Sci. Sports Exerc. 52, 955–967. https://doi.org/10.1249/MSS.0000000000002196.

Casolo, A., Del Vecchio, A., Balshaw, T.G., Maeo, S., Lanza, M.B., Felici, F., Folland, J.P., Farina, D., 2021. Behavior of motor units during submaximal isometric contractions in chronically strength-trained individuals. J. Appl. Physiol. 131, 1584–1598. https://doi.org/10.1152/JAPPLPHYSIOL.00192.2021.

Casolo, A., Maeo, S., Balshaw, T.G., Lanza, M.B., Martin, N.R.W., Nuccio, S., Moro, T., Paoli, A., Felici, F., Maffulli, N., Eskofier, B., Kinfe, T.M., Folland, J.P., Farina, D., Vecchio, A.D., 2023. Non-invasive estimation of muscle fibre size from high-density electromyography. J. Physiol. 601, 1831–1850. https://doi.org/10.1113/JP284170.

Chen, M., Zhou, P., 2016. A novel framework based on FastICA for high density surface EMG decomposition. IEEE Trans. Neural Syst. Rehabil. Eng. 24, 117–127. https://doi.org/10.1109/TNSRE.2015.2412038.

Clancy, E.A., Morin, E.L., Merletti, R., 2002. Sampling, noise-reduction and amplitude estimation issues in surface electromyography. J. Electromyogr. Kinesiol. 12, 1–16. https://doi.org/10.1016/S1050-6411(01)00033-5.

Cohen, J.W., Vieira, T.M., Ivanova, T.D., Garland, S.J., 2023. Differential behavior of distinct motoneuron pools that innervate the triceps surae. J. Neurophysiol. 129 (1), 272–284. https://doi.org/10.1152/jn.00336.2022.

Cudicio, A., Martinez-Valdes, E., Cogliati, M., Orizio, C., Negro, F., 2022. The force-generation capacity of the tibialis anterior muscle at different muscle–tendon lengths depends on its motor unit contractile properties. Eur. J. Appl. Physiol. 122, 317–330. https://doi.org/10.1007/s00421-021-04829-8.

De Luca, C.J., Chang, S.-S., Roy, S.H., Kline, J.C., Nawab, S.H., 2015. Decomposition of surface EMG signals from cyclic dynamic contractions. J. Neurophysiol. 113, 1941–1951. https://doi.org/10.1152/jn.00555.2014.

De Luca, C.J., Erim, Z., 1994. Common drive of motor units in regulation of muscle force. Trends Neurosci. 17, 299–305. https://doi.org/10.1016/0166-2236(94)90064-7.

Del Vecchio, A., Negro, F., Felici, F., Farina, D., 2017. Associations between motor unit action potential parameters and surface EMG features. J. Appl. Physiol. 123, 835–843. https://doi.org/10.1152/JAPPLPHYSIOL.00482.2017.

Del Vecchio, A., Casolo, A., Negro, F., Scorcelletti, M., Bazzucchi, I., Enoka, R., Felici, F., Farina, D., 2019a. The increase in muscle force after 4 weeks of strength training is mediated by adaptations in motor unit recruitment and rate coding. J. Physiol. 597, 1873–1887. https://doi.org/10.1113/JP277250.

Del Vecchio, A., Negro, F., Holobar, A., Casolo, A., Folland, J.P., Felici, F., Farina, D., 2019b. You are as fast as your motor neurons: speed of recruitment and maximal discharge of motor neurons determine the maximal rate of force development in humans. J. Physiol. 597, 2445–2456. https://doi.org/10.1113/JP277396.

Del Vecchio, A., Holobar, A., Falla, D., Felici, F., Enoka, R.M., Farina, D., 2020. Tutorial: Analysis of motor unit discharge characteristics from high-density surface EMG signals. J. Electromyogr. Kinesiol. 53, 102426. https://doi.org/10.1016/J.JELEKIN.2020.102426.

Drost, G., Blok, J.H., Stegeman, D.F., Van Dijk, J.P., Van Engelen, B.G.M., Zwarts, M.J., 2001. Propagation disturbance of motor unit action potentials during transient paresis in generalized myotoniaA high-density surface EMG study. Brain 124, 352–360. https://doi.org/10.1093/BRAIN/124.2.352.

Duchateau, J., Enoka, R.M., 2011. Human motor unit recordings: Origins and insight into the integrated motor system. Brain Res. 1409, 42–61. https://doi.org/10.1016/J.BRAINRES.2011.06.011.

Enoka, R.M., 2019. Physiological validation of the decomposition of surface EMG signals. J. Electromyogr. Kinesiol. 46, 70–83. https://doi.org/10.1016/j.jelekin.2019.03.010.

Farina, D., Fortunato, E., Merletti, R., 2000. Noninvasive estimation of motor unit conduction velocity distribution using linear electrode arrays. IEEE. Trans. Biomed. Eng. 47 (3), 380–388.

Farina, D., Arendt-Nielsen, L., Merletti, R., Graven-Nielsen, T., 2002. Assessment of single motor unit conduction velocity during sustained contractions of the tibialis anterior muscle with advanced spike triggered averaging. J. Neurosci. Methods 115 (1), 1–12.

Farina, D., Merletti, R., Enoka, R.M., 2004. The extraction of neural strategies from the surface EMG. J. Appl. Physiol. 96, 1486–1495. https://doi.org/10.1152/JAPPLPHYSIOL.01070.2003.

Farina, D., Negro, F., Muceli, S., Enoka, R.M., 2016. Principles of motor unit physiology evolve with advances in technology. Physiology 31, 83–94. https://doi.org/10.1152/physiol.00040.2015.

Farina, D., Vujaklija, I., Sartori, M., Kapelner, T., Negro, F., Jiang, N., Bergmeister, K., Andalib, A., Principe, J., Aszmann, O.C., 2017. Man/machine interface based on the discharge timings of spinal motor neurons after targeted muscle reinnervation. Nat. Biomed. Eng. 1 https://doi.org/10.1038/s41551-016-0025.

Felici, F., Del Vecchio, A., 2020. Surface electromyography: What limits its use in exercise and sport physiology? Front. Neurol. 11, 1–6. https://doi.org/10.3389/fneur.2020.578504.

Gallego, J.A., Dideriksen, J.L., Holobar, A., Ibáñez, J., Pons, J.L., Louis, E.D., Rocon, E., Farina, D., 2015. Influence of common synaptic input to motor neurons on the neural drive to muscle in essential tremor. J. Neurophysiol. 113, 182–191. https://doi.org/10.1152/jn.00531.2014.

Gallina, A., Disselhorst-Klug, C., Farina, D., Merletti, R., Besomi, M., Holobar, A., Enoka, R.M., Hug, F., Falla, D., Søgaard, K., McGill, K., Clancy, E.A., Carson, R.G., van Dieën, J.H., Gandevia, S., Lowery, M., Besier, T., Kiernan, M.C., Rothwell, J.C., Tucker, K., Hodges, P.W., 2022. Consensus for experimental design in electromyography (CEDE) project: High-density surface electromyography matrix. J. Electromyogr. Kinesiol. 64, 102656. https://doi.org/10.1016/j.jelekin.2022.102656.

Goodlich, B.I., Del, A., Vecchio, S.A., Horan, J.J., 2023. Kavanagh Blockade of 5-HT 2 receptors suppresses motor unit firing and estimates of persistent inward currents during voluntary muscle contraction in humans. J. Physiol. 601 (6), 1121–1138.

Hassan, A.S., Fajardo, M.E., Cummings, M., McPherson, L.M., Negro, F., Dewald, J.P.A., Heckman, C.J., Pearcey, G.E.P., 2021. Estimates of persistent inward currents are reduced in upper limb motor units of older adults. J. Physiol. 599, 4865–4882. https://doi.org/10.1113/JP282063.

Heckman, C.J., Enoka, R.M., 2012. Motor unit. Compr Physiol 2, 2629–2682. https://doi.org/10.1002/CPHY.C100087.

Heckman, C.J., Enoka, R.M., 2004. Physiology of the motor neuron and the motor unit. Handb. Clin. Neurophysiol. 4, 119–147. https://doi.org/10.1016/S1567-4231(04)04006-7.

Holobar, A., Farina, D., Gazzoni, M., Merletti, R., Zazula, D., 2009. Estimating motor unit discharge patterns from high-density surface electromyogram. Clin. Neurophysiol. 120, 551–562. https://doi.org/10.1016/J.CLINPH.2008.10.160.

Holobar, A., Zazula, D., 2007. Multichannel blind source separation using convolution Kernel compensation. IEEE Trans. Signal Process. 55, 4487–4496. https://doi.org/10.1109/TSP.2007.896108.

Holobar, A., Glaser, V., Gallego, J.A., Dideriksen, J.L., Farina, D., 2012. Non-invasive characterization of motor unit behaviour in pathological tremor. J. Neural Eng. 9 (5) https://doi.org/10.1088/1741-2560/9/5/056011.

Holobar, A., Minetto, M.A., Farina, D., 2014. Accurate identification of motor unit discharge patterns from high-density surface EMG and validation with a novel

signal-based performance metric. J. Neural Eng. 11 (1) https://doi.org/10.1088/1741-2560/11/1/016008.
Hu, X., Suresh, N.L., Jeon, B., Shin, H., Rymer, W.Z., 2014. Statistics of inter-spike intervals as a routine measure of accuracy in automatic decomposition of surface electromyogram. 2014 36th Annu. Int. Conf. IEEE Eng. Med. Biol. Soc. EMBC 2014, 3541–3544. https://doi.org/10.1109/EMBC.2014.6944387.
Hug, F., Del Vecchio, A., Avrillon, S., Farina, D., Tucker, K., 2021. Muscles from the same muscle group do not necessarily share common drive: evidence from the human triceps surae. J. Appl. Physiol. 130, 342–354. https://doi.org/10.1152/JAPPLPHYSIOL.00635.2020.
Inns, T.B., Bass, J.J., Hardy, E.J.O., Wilkinson, D.J., Stashuk, D.W., Atherton, P.J., Phillips, B.E., Piasecki, M., 2022. Motor unit dysregulation following 15 days of unilateral lower limb immobilisation. J. Physiol. 600, 4537–4769. https://doi.org/10.1113/JP283425.
Lulic-Kuryllo, T., Thompson, C.K., Jiang, N., Negro, F., Dickerson, C.R., 2021. Neural control of the healthy pectoralis major from low-to-moderate isometric contractions. J. Neurophysiol. 126, 213–226. https://doi.org/10.1152/jn.00046.2021.
Maathuis, E.M., Drenthen, J., van Dijk, J.P., Visser, G.H., Blok, J.H., 2008. Motor unit tracking with high-density surface EMG. J. Electromyogr. Kinesiol. 18, 920–930. https://doi.org/10.1016/J.JELEKIN.2008.09.001.
Mambrito, B., De Luca, C.J., 1984. A technique for the detection, decomposition and analysis of the EMG signal. Electroencephalogr. Clin. Neurophysiol. 58, 175–188. https://doi.org/10.1016/0013-4694(84)90031-2.
Martinez-Valdes, E., Negro, F., Laine, C.M., Falla, D., Mayer, F., Farina, D., 2017. Tracking motor units longitudinally across experimental sessions with high-density surface electromyography. J. Physiol. 595, 1479–1496. https://doi.org/10.1113/JP273662.
Martinez-Valdes, E., Farina, D., Negro, F., Del Vecchio, A., Falla, D., 2018. Early motor unit conduction velocity changes to high-intensity interval training versus continuous training. Med. Sci. Sports Exerc. 50, 2339–2350. https://doi.org/10.1249/MSS.0000000000001705.
Martinez-Valdes, E., Enoka, R.M., Holobar, A., McGill, K., Farina, D., Besomi, M., Hug, F., Falla, D., Carson, R.G., Clancy, E.A., Disselhorst-Klug, C., van Dieën, J.H., Tucker, K., Gandevia, S., Lowery, M., Søgaard, K., Besier, T., Merletti, R., Kiernan, M.C., Rothwell, J.C., Perreault, E., Hodges, P.W., 2023. Consensus for experimental design in electromyography (CEDE) project: Single motor unit matrix. J. Electromyogr. Kinesiol. 68, 102726. https://doi.org/10.1016/J.JELEKIN.2022.102726.
McManus, L., De Vito, G., Lowery, M.M., 2020. Analysis and biophysics of surface EMG for physiotherapists and kinesiologists: Toward a common language with rehabilitation engineers. Front. Neurol. 11, 1216. https://doi.org/10.3389/FNEUR.2020.576729/BIBTEX.
McManus, L., Lowery, M., Merletti, R., Søgaard, K., Besomi, M., Clancy, E.A., van Dieën, J.H., Hug, F., Wrigley, T., Besier, T., Carson, R.G., Disselhorst-Klug, C., Enoka, R.M., Falla, D., Farina, D., Gandevia, S., Holobar, A., Kiernan, M.C., McGill, K., Perreault, E., Rothwell, J.C., Tucker, K., Hodges, P.W., 2021. Consensus for experimental design in electromyography (CEDE) project: Terminology matrix. J. Electromyogr. Kinesiol. 59, 102565. https://doi.org/10.1016/J.JELEKIN.2021.102565.
Mendell, L.M., 2005. The size principle: a rule describing the recruitment of motoneurons. J. Neurophysiol. 93, 3024–3026. https://doi.org/10.1152/CLASSICESSAYS.00025.2005.
Merletti, R., Cerone, G.L., 2020. Tutorial. Surface EMG detection, conditioning and pre-processing: Best practices. J. Electromyogr. Kinesiol. 54, 102440. https://doi.org/10.1016/J.JELEKIN.2020.102440.
Merletti, R., Farina, A., 2009. Analysis of intramuscular electromyogram signals. Philos. Trans. A. Math. Phys. Eng. Sci. 367, 357–368. https://doi.org/10.1098/RSTA.2008.0235.
Merletti, R., Muceli, S., 2019. Tutorial. Surface EMG detection in space and time: Best practices. J. Electromyogr. Kinesiol. 49, 102363. https://doi.org/10.1016/J.JELEKIN.2019.102363.
Mesquita, R.N.O., Taylor, J.L., Trajano, G.S., Škarabot, J., Holobar, A., Gonçalves, B.A. M., Blazevich, A.J., 2022. Effects of reciprocal inhibition and whole-body relaxation on persistent inward currents estimated by two different methods. J. Physiol. 600, 2765–2787. https://doi.org/10.1113/JP282765.
Nawab, S.H., Chang, S.-S., De Luca, C.J., 2010. High-yield decomposition of surface EMG signals. Clin. Neurophysiol. 121, 1602–1615. https://doi.org/10.1016/j.clinph.2009.11.092.
Negro, F., Muceli, S., Castronovo, A.M., Holobar, A., Farina, D., 2016. Multi-channel intramuscular and surface EMG decomposition by convolutive blind source separation. J. Neural Eng. 13 (2), 026027. https://doi.org/10.1088/1741-2560/13/2/026027.
Ning, Y., Zhu, X., Zhu, S., Zhang, Y., 2015. Surface EMG decomposition based on K-means clustering and convolution kernel compensation. IEEE J. Biomed. Heal. Informatics 19, 471–477. https://doi.org/10.1109/JBHI.2014.2328497.
Nuccio, S., Del Vecchio, A., Casolo, A., Labanca, L., Rocchi, J.E., Felici, F., Macaluso, A., Mariani, P.P., Falla, D., Farina, D., Sbriccoli, P., 2021. Deficit in knee extension strength following anterior cruciate ligament reconstruction is explained by a reduced neural drive to the vasti muscles. J. Physiol. 599, 5103–5120. https://doi.org/10.1113/JP282014.
Okudaira, M., Hirono, T., Takeda, R., Nishikawa, T., Ueda, S., Mita, Y., Holobar, A., Yoshimura, A., Watanabe, K., 2023. Longitudinal development of muscle strength and relationship with motor unit activity and muscle morphological characteristics in youth athletes. Exp. Brain Res. 241 (4), 1009–1019. https://doi.org/10.1007/s00221-023-06590-0.
Oliveira, A.S., Negro, F., 2021. Neural control of matched motor units during muscle shortening and lengthening at increasing velocities. J. Appl. Physiol. 130, 1798–1813. https://doi.org/10.1152/japplphysiol.00043.2021.
Pascoe, M.A., Holmes, M.R., Stuart, D.G., Enoka, R.M., 2014. Discharge characteristics of motor units during long-duration contractions. Exp. Physiol. 99, 1387–1398. https://doi.org/10.1113/EXPPHYSIOL.2014.078584.
Sarto, F., Stashuk, D.W., Franchi, M.V., Monti, E., Zampieri, S., Valli, G., Sirago, G., Candia, J., Hartnell, L.M., Paganini, M., McPhee, J.S., De Vito, G., Ferrucci, L., Reggiani, C., Narici, M.V., 2022a. Effects of short-term unloading and active recovery on human motor unit properties, neuromuscular junction transmission and transcriptomic profile. J. Physiol. 600 (21), 4731–4751. https://doi.org/10.1113/JP283381.
Sarto, F., Valli, G., Monti, E., 2022b. Motor unit alterations with muscle disuse: What's new? J. Physiol. 600 (22), 4811–4813. https://doi.org/10.1113/JP283868.
Sherrington, C.S., 1925. Remarks on some aspects of reflex inhibition. Proc. R. Soc. London. Ser. B Contain. Pap. a Biol. Character 97, 519–545. https://doi.org/10.1098/RSPB.1925.0017.
Škarabot, J., Folland, J.P., Forsyth, J., Vazoukis, A., Holobar, A., Del vecchio, A., 2023. Motor unit discharge characteristics and conduction velocity of the vastii muscles in long-term resistance-trained men. Med. Sci. Sports Exerc. Publish Ah 55 (5), 824–836. https://doi.org/10.1249/MSS.0000000000003105.
Stein, R.B., French, A.S., Mannard, A., Yemm, R., 1972. New methods for analysing motor function in man and animals. Brain Res. 40, 187–192. https://doi.org/10.1016/0006-8993(72)90126-6.
Taylor, J.L., Amann, M., Duchateau, J., Meeusen, R., Rice, C.L., 2016. Neural contributions to muscle fatigue. Med. Sci. Sport. Exerc. 48, 2294–2306. https://doi.org/10.1249/mss.0000000000000923.
Taylor, A.M., Steege, J.W., Enoka, R.M., 2002. Motor-unit synchronization alters spike-triggered average force in simulated contractions. J. Neurophysiol. 88 (1), 265–276.
Valli, G., Sarto, F., Casolo, A., Del Vecchio, A., Franchi, M.V., Narici, M.V., De Vito, G., 2023. Lower limb suspension induces threshold-specific alterations of motor units' properties that are reversed by active recovery. J. Sport Heal. Sci (in press). https://doi.org/10.1016/j.jshs.2023.06.004.
Wood, S.J., Slater, CR., 2001. Safety factor at the neuromuscular junction. Prog. Neurobiol. 64, 393–429. https://doi.org/10.1016/S0301-0082(00)00055-1.